Experimental research on sliding bubble diameter and velocity in a narrow rectangular channel under natural circulation condition

YAN Meiyue[1], YAN Changqi[1], REN Tingting[1], YANG Yongyong[2], CHEN Kailun[1], ZHANG Rui[1], and YANG Kuan[1]

1. *Fundamental Science on Nuclear Safety and Simulation Technology Laboratory, Harbin Engineering University, Harbin 150001, China (yanmeiyue@hrbeu.edu.cn; changqi_yan@163.com)*
2. *China Nuclear Power Operation Technology Corporation, LTD, Wuhan 430074, China*

Abstract: Heat transfer enhancement by the behaviors of the bubbles sliding along the heating surface is studied by visual experiments by a high-speed digital camera to observe the bubble behaviors in subcooled flow boiling in a narrow rectangular channel under natural circulation. A sequence of image processing algorithms was used to deal with the original bubble images to get relevant bubble parameters, including bubble diameter and bubble velocity, *etc.* The experiments were performed at pressures ranging from 0.2 MPa to 0.4 MPa, with inlet subcooling ranging from 20 to 60 K and heat flux ranging from 100 kW/m^2 to 300 kW/m^2. We found that almost all the bubbles will slide along the heating wall. In each operating condition, the bubble diameter distribution approximately conforms to lognormal distribution while the bubble velocity distribution agrees well with normal distribution. Moreover, local thermal hydraulic parameters have significant influences on the stochastics and mean characteristics of the bubble. The present experiment data shows a good linear relationship between the mean velocity and mean diameter of sliding bubbles, and the correlation for the mean diameter was obtained by the multivariate analysis method. Besides, the experimental phenomenon shows that the bubble diameter and velocity oscillate simultaneously under natural circulation when the inlet subcooling is 40K and the heat flux exceed 200 kW/m^2.

Keywords: narrow rectangular channel; natural circulation; sliding bubble; bubble diameter; bubble velocity

1 Introduction

More attention has been attracted for narrow channel for their great improvements on the capability of heat transfer compared with the conventional channel. Kandlikar [1] regarded a gap size between 1 mm and 3 mm as a narrow channel, and as a matter of fact, the narrow rectangular channel is widely used in many industry fields, such as heat exchangers and the reactor core of the barge-mounted nuclear power plants [2]., where heat transfer enhancement by the behaviors of the bubbles sliding along the heating surface has been reported by many researchers in recent years.

The main purpose of present work is to investigate bubble behaviors in upward subcooled flow boiling in a vertical narrow rectangular channel under natural circulation. In the subsequent part of this paper,

overview of the past studies is first reviewed, Then experimental method used in this study is introduced for the visual observation of the bubble characteristics such as bubble diameter, bubble velocity, bubble growth rate. Finally the effects of the major thermal hydraulic parameters on bubble parameters.

2 Past experimental studies on characters of bubble behaviors in a narrow rectangular channel

Various researches show that the bubble behaviors in a narrow rectangular channel is distinctly different from that of a convectional channel due to confined geometry [3-12].

Okawa *et al.* [3, 4] studied bubble behaviors in vertical narrow rectangular channel. The following three different bubble rise paths were observed after the departure from a nucleation site: (i) some bubbles slid along the vertical heating wall for a long distance, (ii) some bubbles disappeared due to the

Received date: August 28, 2018
(Revised date: September 23, 2018)

condensation of subcooled liquid, and (iii) some bubbles might reattach to the heating wall.

Li *et al.* [5] focused on the behaviors of sliding bubble in a vertical narrow rectangular channel. Two kinds of sliding bubble were observed in the experiment. The velocity and diameter of some bubbles changed quickly and had shorter lifetime, while the other bubbles survived for a long time and their velocity and diameter were approximately unchanged.

Those two kinds of sliding bubble were also found in the study of Junsoo *et al.* [6]. They also conducted on experiments to further study the influence of thermal parameters on bubble behaviors. The results showed that: (i) at low mass fluxes (*i.e.*,140 and 280 kg/(m^2 s)), more bubbles grew fast near the nucleation site, then shrank subsequently, and (ii) sliding bubble preferred to grow steadily as mass flux increased (*i.e.*, 420 kg/(m^2 s)).

According to the work by Yuan [7, 8], the sliding bubbles enhanced the wall heat transfer and that the system pressure has the significant effects on the heat transfer through the impacts on bubble behaviors.

The mechanism of sliding bubble behaviors was visually studied by Xu *et al.*[9-11]. They found that the sliding bubbles were in spherical shape according to the observation from the wide side of the narrow rectangular channel. The sliding bubble velocity increases with increasing bubble diameter and liquid flow rate. However, the velocity is less than local liquid velocity at the initial moment, and it will exceed the local liquid velocity with time going.

Yang *et al.* [12] found that sliding bubble velocity approximately conformed to a normal distribution, and the bubble sliding velocity increase with the increase of its diameter.

Puli [13] conducted on experiments to study the influence of pressure on bubble diameter distribution, and the results showed that the quantity of smaller bubbles increases with the increase of pressure.

In Maurus's work [14], it was also found that the heat flux and liquid mass flow rate affect the bigger bubbles more obviously, while have little effect on the smaller bubbles.

For the studies associated with bubble diameters, the work concerning the bubble departure diameter is abundant. In a work by Zeng [15], a forced convection boiling facility has been fabricated in which bubble departure can be investigated. Their analytical results show the influence of liquid velocity and wall superheat on bubble departure diameters. Klausner [16] and Thorncroft [17] further studied and proposed a model in a detailed analysis of various acting on growing and sliding bubbles for predicting bubble detachment diameters and sliding trajectories.

Starting from the model proposed by Klausner [16], an improved force-balance model of bubble departure in forced convection boiling has been developed by Colombo [18] , where modifications were made on the correlation of surface tension force and a new equation governing bubble growth considering condensation on the bubble cap.

However, few studies focus on the distribution and mean characteristics of bubble parameters, which also have a significant influence on the analysis of boiling heat transfer and the building of wall heat flux partitioning model. Therefore, Zeitoun *et al.* [19] visually investigated on the bubble behaviors in subcooled flow boiling of a vertical annular channel under low pressure and mass flux condition, where the mass flux, heat flux and subcooling were found to have significant effects on mean bubble size. They also reduced a correlation to model the mean bubble diameter with those observed parameters mentioned above.

However, the bubble characteristics for natural circulation flow in a vertical narrow rectangular channel are still unknown, although many researches have been performed in narrow rectangular channels. Natural circulation flow is driven by the density difference between the riser and down-comer in some operational condition of nuclear reactor, *e.g.* a safety related operational event [20], and the reactor coolant through the core by natural circulation [21]. Such systems enhance safe operational potential and reliability compared to pumped systems. Therefore,

the study of bubble behaviors is needed to meet the purpose of understanding the boiling heat transfer mechanism under natural circulation condition.

3 Experimental methods

3.1 Description of the experimental facility

An experimental loop as shown in Fig.1 was designed and constructed for the study on the characteristics of bubble in a narrow rectangular channel under natural circulation. The experimental loop is mainly composed of a primary loop, an auxiliary loop, and a visualization part.

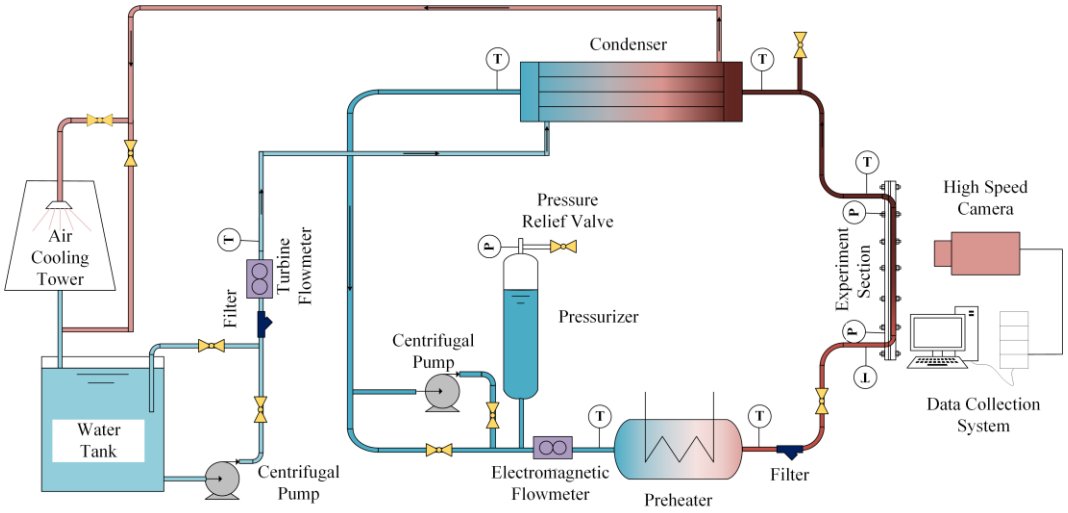

Fig.1 Schematic diagram of experimental loop.

The primary loop mainly consists of four major parts, including a pressurizer, a preheater, a test section, and primary side of condenser. The pressurizer is connected with a nitrogen bottle to maintain the system pressure in loop. The fluid is preheated to the projected temperature firstly in the 45 kW preheater, and then injects to the test section for subcooled flow boiling experiments. A DC power supply with a capacity of 2000 A/50 V is adopted to provide a wide range of heat flux to the test section. After the fluid leaving from test section, the temperature is reduced to a subcooled state at the condenser before returning to the pump in primary loop.

The auxiliary loop is composed of a water tank, a cooling tower, a centrifugal pump and secondary side of condenser. The function of auxiliary loop is to provide cooling water to cool the working medium from superheated state to subcooled state, and to ensure the subcooled flow boiling which is certain to occur in the test section.

Visualization experimental system is achieved from the direction of wide side of the channel as shown in Fig. 2. A FAST-CAM SA5 high-speed digital camera and a 105mm F2.8 macro lens are used to record the bubble behaviors. The frame rate is set to 5000 fps and the corresponding viewing area is about 20 × 20 mm^2 in this study. In order to clearly record the bubble behaviors, two fiber lamps (power level adjustable within 0-150W) are utilized to provide sufficient illumination for the filming. The camera and fiber lamps are fixed on a 2-D guide rail, and the camera is able to move horizontally and vertically.

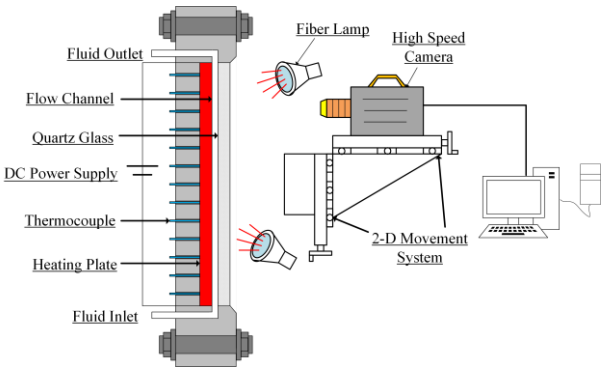

Fig.2 Schematic of visualization system.

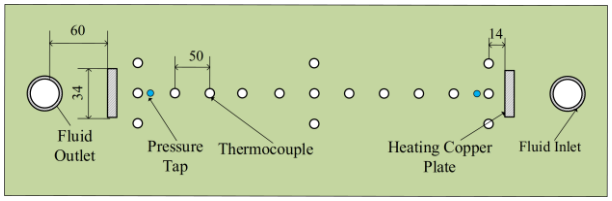

Fig. 3 Arrangement of temperature measuring points.

To enable visualization of the bubble behaviors, the channel is designed to be single-side heated. The total heating length is 550 mm. The temperature is measured by N-type shielded thermocouples, and the pressure is measured with pressure transducers at the inlet and outlet of the test section. There are totally 17 measuring points to measure the heating plate temperature distribution along the flow channel. The arrangement of temperature distribution points along the flow channel is illustrated in Fig. 3.

3.2 Experimental conditions and procedure

Deionized water is used as working fluid in this study. To avoid the effect of dissolved non-condensable gases in the water on experimental phenomena, eliminating non-condensable gas before the experiment is necessary. For the sake of reducing the solubility of the incondensable gas in the fluid, the cooling water loop is cut off and the deionized water is heat up to saturate boiling state at the exit of the test section. The non-condensable gas is released from the water experimental loop through the venting valve located at the top of the circulation loop. The degassing process can be checked by observing the bubbles generation locations and the sizes in the test section. Bubbles generated by non-condensable gases are much smaller than that generated at heating surface. When subcooled boiling occurs in the test section, there is no bubble generated at the inlet of test section until satisfactory degassing level.

After degassing, auxiliary cooling loop is activated to create density difference between the riser and down-comer of primary loop. Then centrifugal pump is shut off to switch the working mode from forced circulation to natural circulation. The main experimental parameters are system pressure, fluid subcooling, heat flux and mass flux. When a steady state is reached (the change of temperature less than 0.2℃), the bubble images and thermal hydraulic data are collected simultaneously. Main experimental parameters are summarized in Table 1.

Table 1 Experimental parameter ranges

Experimental parameter	Range
System pressure (P_{sys})	0.2-0.4 MPa
Inlet fluid subcooling ($\Delta T_{in,sub}$)	20-60 K
Heat flux (q)	100-300 kW/m^2
Mass flux (G)	280-450 kg/(m^2 s)

3.3 Experimental data processing methods

Massive amounts of bubble image data were obtained in the experiment. Therefore, a batch-processing method was developed to deal with the bubble images. Pre-processing of bubble images is made by Image Pro Plus 6.0, and a sequence of digital image processing algorithms is applied to deal with the original video to extract bubble location and shape information. From the results of image processing, bubble diameter and bubble velocity of each frame existed in the filming window are obtained.

Xu *et al.* [11] and Yang *et al.* [23] investigated experimentally on the bubble behavior from the wide side and gap side of the narrow rectangular channel simultaneously, and they found that the shape of bubble is approximately spherical. By the authors' experiments, the bubbles are not confined by the wall of a narrow rectangular channel whose gap size is 2 mm. So the bubble diameter measured from wide view is used to represent the equivalent diameter of bubble. However, the shape of bubble is elongated in the direction normal to the heating wall due to the existence of fluid flow and heating wall. Therefore, the equivalent bubble diameter can be calculated as the mean value of all bubble diameters measured at 2° intervals (the total is 90 groups) as can be written as Eq. (1),

$$D_e = \sum_{1}^{90} D_i \Big/ 90 \tag{1}$$

The bubble velocity is calculated according the bubble locations in successive images. It can be seen from the video record by high-speed camera so that the bubble movement in horizontal direction can be negligible compared with that in vertical direction. Threfore the velocity of the centroid of a bubble can be calculated as

$$v_e = \frac{y_{t_2} - y_{t_1}}{t_2 - t_1} C \tag{2}$$

where y is the bubble coordinate in vertical flow direction; t_2-t_1 denotes the time internal of two images.

The following equations can be obtained for the mean diameter and mean velocity of a large number of bubbles during the shooting time,

$$D_{ave} = \frac{1}{\sum_{i=1}^{m} n_i}\left(\sum_{i=1}^{m}\sum_{j=1}^{n_i} D_{e,j}\right) \quad (3)$$

$$v_{ave} = \frac{1}{\sum_{i=1}^{m} n_i}\left(\sum_{i=1}^{m}\sum_{j=1}^{n_i} V_{e,j}\right) \quad (4)$$

where D_{ave} and v_{ave} are the average diameter and velocity of the bubble in the filming window; m represents the number of frames, and n_i represents the number of bubbles at each frame.

The temperature gradient normal to the heating plate is almost normal to the heating plate because the test section is well thermally isolated and the heating plate is only 3 mm. Therefore, the situation is considered as one-dimensional steady state heat conduction problem.

$$q = \frac{Q}{W \cdot L_{tot}} \quad (5)$$

$$T_{w,in} = T_{w,out} - \frac{q\delta}{2k} \quad (6)$$

where W, L_{tot}, δ is the width, length, thickness of heating plate, respectively, k is the heat conductivity coefficient of heating plate.

3.4 Uncertainty analysis

The measurement accuracies of thermal parameters and bubble parameters are crucial for the reliability of the subsequent analysis. Some thermal parameters are directly measured including wall temperature, pressure, current, voltage, *etc*. The errors of those parameters are usually determined by the characteristics of measurement instruments themselves. The accuracies of those direct measured parameters are presented in Table 1. While indirect measured parameters are needed to calculate by some basic measurement values. The uncertainties of those parameters can be estimated by the following Kline-McClintock method [24]

$$\sigma_y = \pm\sqrt{\sum_{i=1}^{n}\left(\frac{\partial y}{\partial x_i}\sigma_i\right)^2} \quad (7)$$

where the y is a function of variables x_1, x_2, x_3... x_n, σ_y and σ_i are the uncertainties of y and x_i, respectively.

In the experiment, the filming frame rate and resolution are set to 5000 fps and 1240×1240 pixels. The corresponding physical scale of the view window is about 20×20 mm^2. Since the uncertainty for locating the position is within ±2 pixels, the maximum error of bubble location is limited to ±0.04 mm. The uncertainties of main parameters are summarized in Table 2.

Table 2 Uncertainties of main parameters

Measured parameters	Maximum error (+/-)
Time	10^{-6} s
Length	0.5 mm
Heat flux	0.5%
Wall temperature	0.56 K
Calibration of the image	0.016 mm/pixel
Bubble location	0.04 mm
Bubble diameter	0.08 mm
Bubble velocity	0.04 m/s

4 Results and discussions

When subcooled flow boiling occurs, large amounts of bubbles are generated on the heating surface, and the bubbles have influences on each other. The research on the growth characteristics of a single bubble is not enough to reflect the overall characteristics of bubble group. Therefore, to establish a more accurate boiling heat transfer model, it is necessary to study the bubble group behaviors.

The authors of this paper conducted on a series of experiments to observe the effects of subcooling and heat flux on the bubble group behaviors. The experimental conditions are shown in Table 3, where height H represents the distance between the shooting position of high-speed camera lens and the lower side of the rectangular channel.

Table 3 Experimental conditions

EXP.	Height H / mm	Heat flux q / (kW/m^2)	Inlet subcooling $\Delta T_{in,sub}$/K
A	468	160.8	40.8
B	185	160.0	40.8
C	468	202.8	40.8
D	468	161.5	60.9

A batch-processing method was developed to deal with the original bubble images to get more intuitive bubble behaviors images. Figure 4 shows the processed images of bubbles in the window under the

four different experimental conditions. It can be seen from Fig. 4 that there are large differences in the sizes and the number of bubbles under different conditions. At the same time, due to the difference of bubbles growth characteristics, the bubbles diameters are diverse even under same experimental conditions.

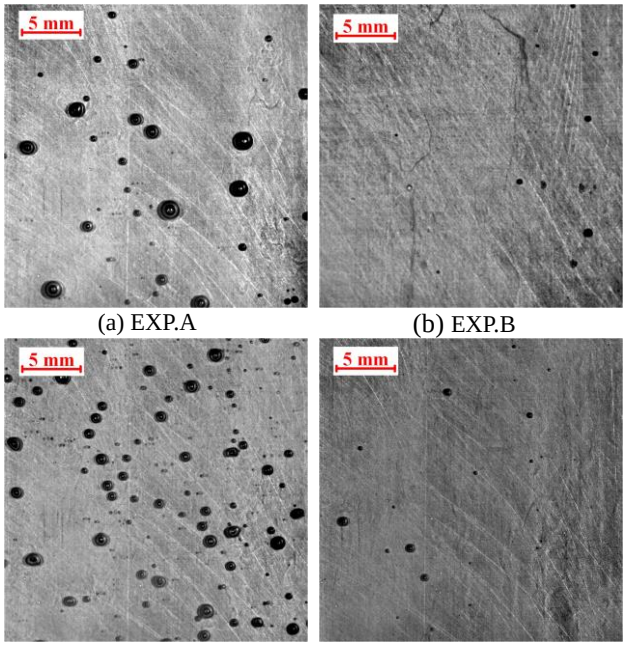

(a) EXP.A (b) EXP.B

(c) EXP.C (d) EXP.D

Fig. 4 Bubble behaviors in a narrow rectangular channel under natural circulation.

In subcooled flow boiling, the bottom of the bubble is located at the heating wall and the top of the bubble is in the subcooled fluid. The number of nucleation sites on the heated wall mainly depends on the superheat of the heating wall. The size of bubbles is related to the evaporation rate at bubble bottom and the condensation rate at bubble top.

By the comparison between Fig. 4 (a) and (b), it can be found that the sizes and the number of bubbles increase significantly along the flow direction. In working condition of B, the local wall superheat is low and the local liquid subcooling is large due to the heating distance of along the wall is short. The superheat is not enough to active many nucleation sites to generate many bubbles, and the high subcooling will significantly decrease the bubble size. Therefore, the number and the size of bubble will increase with increasing vertical height.

From the comparison of Fig. 4 (a) and (c), it can be realized that the increase in heat flux will cause the boiling on the heating wall to be more intense, and increase the number and the size of bubbles. This is because an increase in heat flux will increase the wall superheat, then active more nucleation sites and lead to more bubbles generate on heating surface. At the same time, the local subcooling of the mainstream liquid decreases.

As a result, the evaporation rate at the bottom of the bubble will increase while the condensation rate at the top decrease, will lead to an increase of bubble diameters. The differences of bubble behaviors obtained from Fig. 4 (a) and (d), it can be seen that the number and size of bubbles decrease as the subcooling increases, while the change of bubble sizes is small. This phenomenon is because the liquid subcooling itself will not directly affect the generation of bubbles.

In summary, the inhomogeneity of the temperature field on the heating surface and the complex interplay between the bubbles make characteristics of the bubbles complicated in the narrow channel.

4.1 The distribution characteristics of sliding bubbles

From the experimental phenomenon, it can be seen that the sliding bubble diameter and speed is diverse even under the same operating conditions. The bubble diameters generated at different nucleation sites are different, and even generated at the same sites also different growth characteristics per frame during the growth process. The distribution characteristics of sliding bubble diameter and velocity are illustrated in Figs. 5-7. As shown in those figures, both the bubble diameter and velocity cover a wide range, and the distribution of sliding bubble diameter approximately conforms to a lognormal distribution, while the velocity approximately conform to a normal distribution.

The two functional forms can be written as

$$p(x)=\left(\sqrt{2\pi}\sigma x\right)^{-1}\exp\left[-\frac{1}{2\sigma^2}\left(\ln x-\mu\right)^2\right] \quad (8)$$

$$f(x)=\left(\sqrt{2\pi}\sigma x\right)^{-1}\exp\left[-\frac{1}{2\sigma^2}\left(x-\mu\right)^2\right] \quad (9)$$

The confined bubbles in the narrow rectangular channel with 2 mm in gap are not observed in this experiment. The bubble diameters are mainly concentrated between 0.2 mm-1 mm. The bubble sliding velocity are less than 1 m/s, and mainly concentrated between 0.2 m/s-0.5 m/s.

From Fig. 5, it can be seen that the maximum value and standard deviation of the diameter and velocity distributions increase along the flow direction. This indicates that more bubbles with large diameter generate at the top of the heating plate. At the same time, the bubble sliding velocity generally increases with increasing diameter. This is because the bubble size affects the drag force on it, which leads to an increase in bubble velocity.

Figure 6 shows that the distribution standard deviations of bubble diameter and velocity increase with the increase of heat flux. This phenomenon means that the increase of heat flux not only promotes the larger bubble generate in the channel, but also benefits the survival of small bubbles, and the changes of bubble diameters will affect the bubble velocity.

It can be seen from the Fig. 7 that the change of distributions of sliding bubble diameter and velocity is not obvious when the inlet subcooling changes from 40 K to 60 K. That is because the number of bubble generation mainly depends on the wall superheat. The subcooled liquid flows through the heating wall, and reduces the wall superheat, resulting in a significant reduction of bubbles generated on the wall.

The bubble diameter depends on both of the wall superheat and liquid subcooling. When the subcooling of mainstream liquid is high, the change of wall superheat is not the main factor affecting bubble growth. The subcooling of both 40 K and 60 K have enough ability to reduce the diameters of bubble generated at the wall to a similar value.

Moreover, the bubble sliding velocity and diameter have same trend. Therefore, the distributions of bubble diameter and velocity are almost unchanged although the bubble number changes when the subcooling changes from 60 K to 40 K.

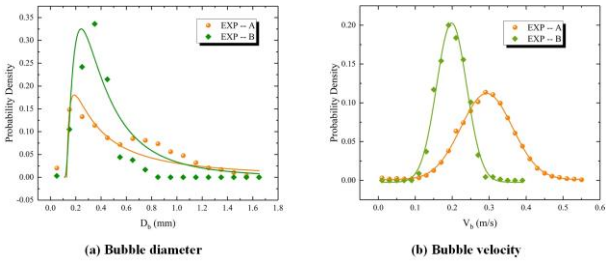

Fig. 5 Effect of vertical height on bubble parameters.

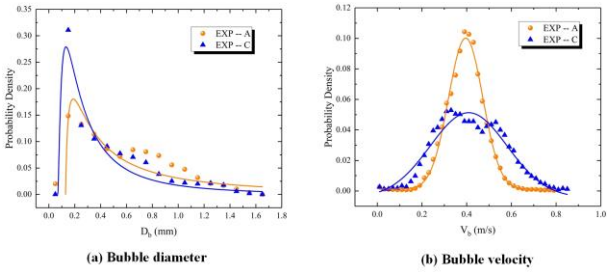

Fig. 6 Effect of heat flux on bubble parameters.

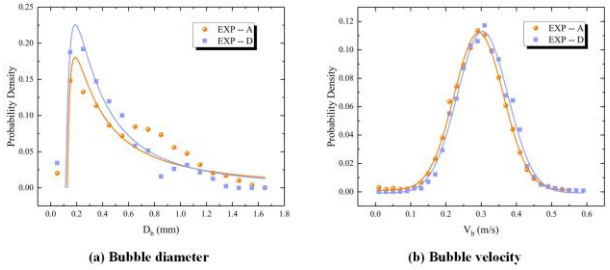

Fig. 7 Effect of subcooling on bubble parameters.

4.2 The mean characteristics of sliding bubbles

4.2.1 Effects of thermal parameters on mean diameter of sliding bubble

The distribution characteristic of sliding bubble parameters from the previous studies gave the following observations: To better understand the group behavior of sliding bubble, the bubble mean characteristic is obtained. The effect of inlet subcooling on bubble mean diameter is as shown in Fig. 8.

It is found that the sliding bubble diameter decreases with the increasing inlet subcooling, and this may be attributed to the following reasons: The condensation process existed on the top of the bubble is strengthened due to the increase of the bulk fluid subcooling. In addition, the specific volume of the fluid decreases with increasing inlet subcooling, resulting in the increase of fluid velocity under

constant mass flow rate. As a result, the superheat of heating wall decreases, thus the evaporation rate at the bottom of a bubble decrease. Both factors above are not beneficial to the bubble growth process, which can result in smaller bubble size. It is found that the bubble mean diameter is almost unchanged when the subcooling changes from 40 K to 60 K, which is consistent with the analysis of the distribution characteristics of bubbles.

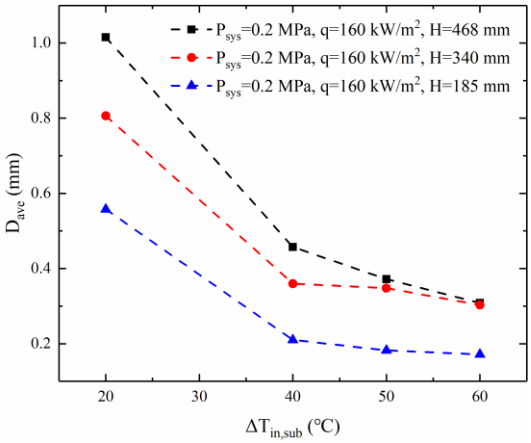

Fig. 8 Effect of inlet subcooling on mean diameter.

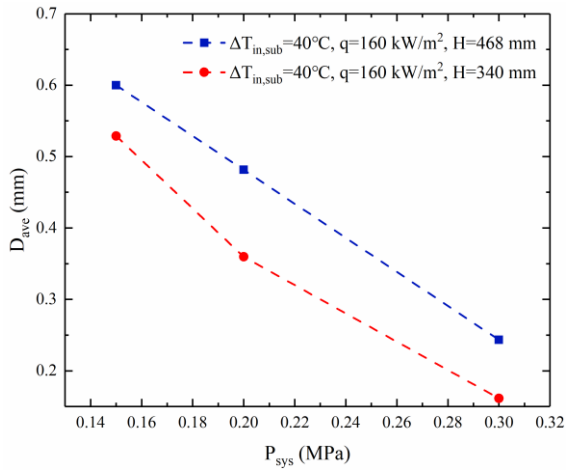

Fig. 9 Effect of pressure on mean bubble diameter.

The bubble mean diameter under different pressure is depicted in Fig. 9. As seen in Fig.9, the pressure has significant effect on sliding bubble diameter. Many studies focusing on bubble behaviors have shown that bubble behaviors depend on the forces on bubbles. In terms of the forces on the bubble, the unsteady drag force acting on bubbles attributed to the asymmetric growth of bubbles which is much greater than other forces in a narrow rectangular channel [7].

The component of this force is in the direction normal to the heating surface, which makes the bubble more inclined to attach on the nucleation site and grow. The surface tension of the bubble is also related to the pressure. Under low pressure, the unsteady drag force and the surface tension are large, both of which contribute to bubble grow at its nucleation site for a long time. When under higher pressure, the two forces are much smaller, which lead to bubble departure from its nucleation site very easily. If the bubble would detach from the heating wall, then the evaporation rate at the bottom of the bubble will be reduced, resulting in a decrease in bubble diameter. Therefore, the bubble diameter will decrease as the pressure increases.

4.2.2 The correlation to predict the mean diameter

The bubble behavior and mean diameter are driven by the need to understand the physical phenomena associated with subcooled flow boiling in narrow channel under natural circulation. The model proposed by Zeitoun [19] is widely used to predict the average diameter of sliding bubbles in concentric annual test section. In his analysis, a dimensionless diameter form can be calculated by the following equation:

$$\frac{D_{ave}}{\sqrt{\sigma / g\left(\rho_l - \rho_v\right)}} = \frac{0.0683\left(\rho_l / \rho_v\right)^{1.326}}{\mathrm{Re}^{0.324}\left(Ja + \dfrac{149.2\left(\rho_l / \rho_v\right)^{1.326}}{Bo^{0.487}\,\mathrm{Re}^{1.6}}\right)} \quad (10)$$

The comparison between the correlation proposed by Zeitoun and the present experimental data is shown in Fig. 10. From this figure, it can be seen intuitively that the value of average diameter predicted by Zeitoun model is generally larger than the experimental value. The reason is because his model is assumed to be for vertical annular channel under forced circulation without considering the characteristics of bubble behavior in narrow rectangular channel under natural circulation.

In this study of the average bubble diameter, the influences of thermal hydraulic parameters and narrow rectangular channel are analyzed. And it was found that the liquid subcooling, wall superheat, pressure and the gap size of narrow channel are the main influencing factors of mean bubble diameter,

and it is assumed that the effects of these factors on bubble diameter are independent.

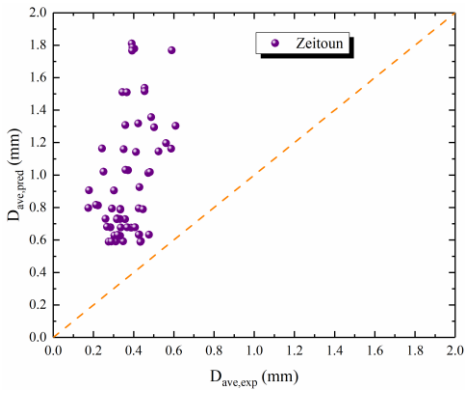

Fig. 10 Comparison between Zeitoun's model and experimental data.

Thus, the mean bubble diameter in narrow rectangular channel can be expressed by the following pure empirical correlation:

$$D_{ave} = k \cdot Ja^{a} \cdot Bo^{b} \cdot Re^{c} \cdot \theta^{d} \left(\frac{\varepsilon}{La}\right)^{e} \tag{11}$$

$$Ja = \frac{\rho_l C_{pl} \Delta T_w}{\rho_v h_{fg}} \quad Bo = \frac{q}{G h_{fg}} \quad Re = \frac{vl}{\upsilon} \quad \theta = \frac{T_w - T_f}{\Delta T_w}$$

where C_{pl}: liquid specific heat capacity in kJ/(kg·℃), h_{fg}: latent heat of vaporization in kJ/kg, ΔT_w : wall superheat in K, G: mass flow rate in kg/s; q: heat flux, in kW/m^2, v: liquid velocity in m/s, υ: kinematic viscosity in m^2/s, T_w, T_f : wall and fluid temperature in K, respectively, ε: the narrow gap width of rectangular channel.

In the prediction correlation given by Eq. (11), we introduce Ja to describe the influence of wall superheat and pressure on the growth of bubbles. The parameter Bo and Re are introduced here to reflect the effect of liquid flow on bubble diameter. In fact, the balance of the evaporation rate at the bubble bottom microlayer and the condensation rate at the bubble top determines the bubble growth. However, the wall superheat and liquid subcooling change simultaneously with the variation of operating conditions.

It is difficult to study a single effect of wall superheat or liquid subcooling on bubble diameter. Therefore, the dimensionless parameter θ is introduced to consider the difference of wall superheat and liquid subcooling simultaneously. The last term ε/La in Eq. (11) considers that the bubble growth is influenced by the limitation of narrow rectangular channel. $La = \sqrt{\sigma / g\left(\rho_l - \rho_v\right)}$, and La is the Laplace number.

With the method of multiple linear regression, the bubble mean diameter in a narrow rectangular channel under natural circulation condition can be calculated as

$$D_{ave} = 1.9491 \times 10^{6} \cdot Ja^{-0.73318} \cdot Bo^{-0.50145} \cdot \mathrm{Re}^{-1.50351} \cdot \theta^{-0.23428} \left(\frac{\varepsilon}{La}\right)^{-18.91624} \tag{12}$$

Figure 11 shows the comparison between the predicted values of bubble mean diameters and the experimental values. The comparison results show that the errors of most experimental data are less than ±30%. Therefore, within the range of experimental conditions, the calculated expression put forward in Eq. (12) can be used for the prediction of bubble mean diameter.

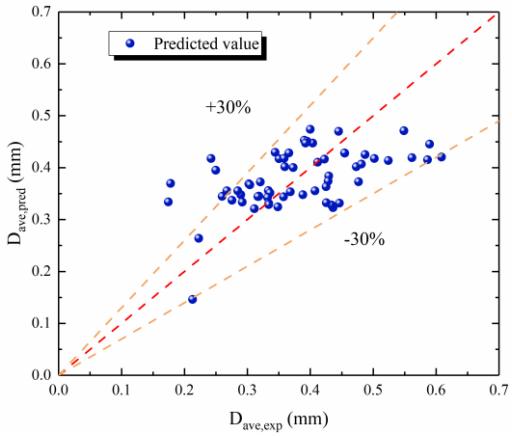

Fig. 11 Comparison between predicted values and experimental values.

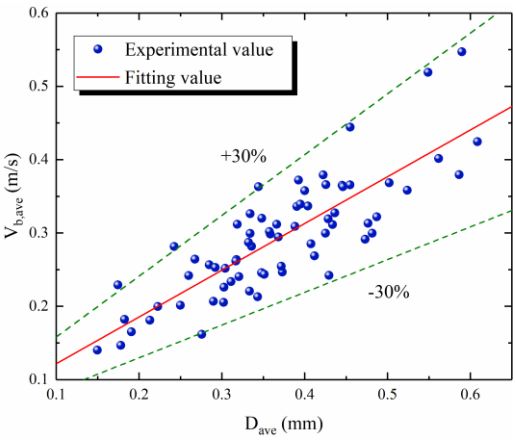

Fig. 12 The relationship between sliding bubble mean velocity and mean diameter.

4.2.3 The correlation between sliding bubble mean diameters and mean velocity

From the above research results, it can be seen that the bubble diameter and bubble velocity have the same changing trend with the change of thermal parameters. So it is reasonable to assume that there is a certain relation between the two bubble parameters.

The correlation between average bubble velocity and diameter under different conditions is shown in Fig. 12. According to the analysis of the previous research results and this figure, it can be seen intuitively that the bubble mean velocity is linearly related to the mean diameter. This phenomenon can be explained as that the increased bubble diameter can result in a larger drag force acting on the bubble which can cause an acceleration of bubble velocity. In addition, during the shooting time of 0.2 ms, the mass flow rate in the test section does not change. With increasing bubble diameter, the cross section average density start to decrease. Then the liquid flow velocity increases, resulting in an increase of bubble velocity.

4.2.4 The phenomenon of bubble oscillation

When the heat flux exceeds 200 kW/m^2 and the inlet liquid subcooling is 40 K, almost all the bubbles are observed to oscillate in the channel. The vibrations of the average bubble diameter and velocity over time are shown in Fig. 13. The value of each point in the graph represents the average of all the captured bubbles in 10 continuous frames. It can be seen from Fig. 13 (a) and (b) that the phase difference of bubble diameter and velocity is so little that it can be neglected. So the bubble parameters oscillate almost simultaneously, and its frequency is fairly regular about 10 Hz.

This phenomenon can be explained as the larger of heat flux, the more intense of boiling is, which will lead to decreases of density in the test section, resulting in an increase of density difference between riser and down-comer in experimental loop. It will increase the driving force of natural circulation, and finally the increases of mass flow rate. As boiling heat transfer increases with the increase in mass flow rate, the wall superheat decreases, the evaporation rate at the bubble bottom decreases.

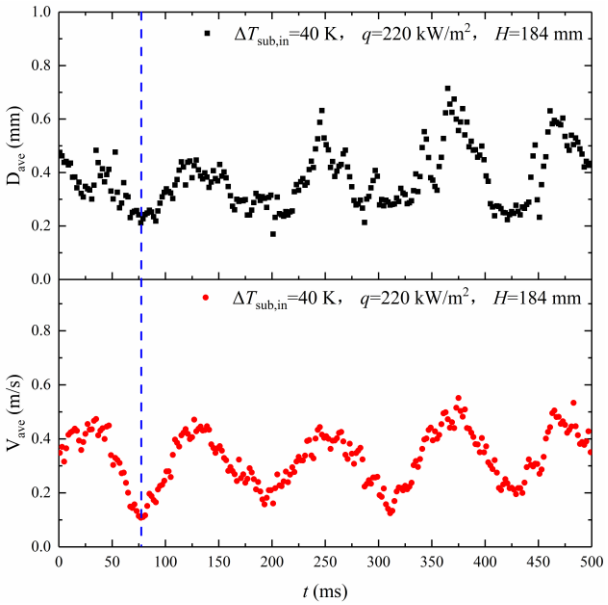

(a) H=184 mm

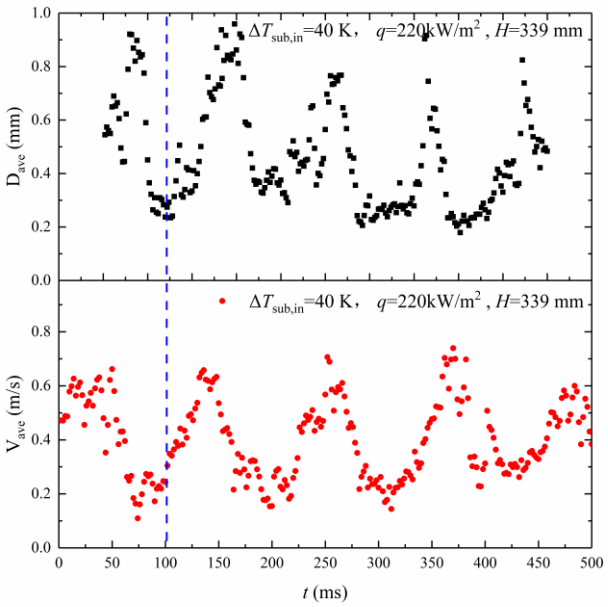

(b) H=339 mm

Fig. 13 The characteristic of bubble oscillation.

Those result in a decrease in bubble diameters. According to the previous analysis, there is a good linear relationship between the bubble velocity and the bubble diameter, so the bubble velocity changes synchronously. Comparison of Fig. 13 (a) and (b) can be concluded that as the amplitude increases with the increasing height in the channel when the other experimental conditions are the same. That is because under the same inlet thermal parameters, the boiling is more intense along the test section, which leads to the phenomenon above more obviously.

5 Conclusions

In this paper the visualization experiment was conducted to observe the characteristics of bubble behavior in subcooled flow boiling in a narrow rectangular channel under natural circulation. A high-speed digital camera was used to record the bubble behaviors, and bubble parameters were obtained through a series of image processing methods. Relevant thermal hydraulic parameters were collected by data acquisition system synchronously. In the research the following conclusions can be drawn:

1) The sliding bubble diameter and velocity approximately follow lognormal distribution and normal distribution, respectively. The standard deviations and maximum values increase along the flow direction and crease with increasing heat flux and decreasing inlet subcooling.
2) The mean diameter of sliding bubbles continues to decrease with increasing inlet subcooling and system pressure, and the bubble average velocity is linearly related to the average diameter under experimental conditions. After considering the main influencing factors of bubble diameters comprehensively, a model to predict the sliding bubble mean diameter was proposed.
3) When inlet liquid subcooling is 40K and heat flux exceeds about 200 kW/m^2, it can be found that bubble diameters and velocities oscillate synchronously in a narrow channel under natural circulation.

Nomenclature

D bubble diameter, m
T temperature, ℃
H height, m
S shooting area, m^2
W width of the channel, m
L length of the channel, m
P pressure, Pa
G mass flow, kg/m^2 s
C_{pl} liquid specific heat transfer, J/kg ŧK
h_{fg} latent heat of vaporization, J/kg
t time, s
v bubble velocity, m/s
q heat flux, kW/m^2
m number of frames
n number of bubbles
k heat conductivity coefficient, W/m ŧK
Re Reynolds number
Ja Jakob number
Bo Boiling number
La Laplace number

Greek symbols

σ uncertainty
δ thickness of heating plate
θ dimensionless parameter
υ kinematic viscosity
ρ density
ε narrow gap size of channel
σ surface tension coefficient

Subscripts

ave average value
tot total
in inlet
out outlet
l liquid
v vapor
sub subcooling
b bubble
w wall
e equivalent

Acknowledgments

The authors greatly appreciate the support of Natural Science Foundation of China (Grant No.11675045).

References

[1] KANDLIKAR, S.G.: Two-phase flow patterns, pressure drop, and heat transfer during boiling in minichannel flow passages of compact evaporators. HEAT TRANSFER ENG 2002; 23: 5-23.
[2] TIAN, C., YAN, M., WANG, J., CAO, X., YAN, C., and YU, S.: Experimental investigation of flow and heat transfer for natural circulation flow in an inclined narrow rectangular channel. PROG NUCL ENERG 2017.
[3] OKAWA, T., ISHIDA, T., KATAOKA, I., and MORI, M.: An experimental study on bubble rise path after the departure from a nucleation site in vertical upflow boiling. EXP THERM FLUID SCI 2005; 29: 287-94.
[4] OKAWA, T., ISHIDA, T., KATAOKA, I., and MORI, M.: Bubble rise characteristics after the departure from a nucleation site in vertical upflow boiling of subcooled water. NUCL ENG DES 2005; 235: 1149-61.
[5] LI, S., TAN, S., XU, C., GAO, P., and SUN, L.: An experimental study of bubble sliding characteristics in narrow channel. INT J HEAT MASS TRAN 2013; 57: 89-99.

[6] YOO, J., ESTRADA-PEREZ, C.E., and HASSAN, Y.A.: Experimental study on bubble dynamics and wall heat transfer arising from a single nucleation site at subcooled flow boiling conditions–Part 2: Data analysis on sliding bubble characteristics and associated wall heat transfer. INT J MULTIPHAS FLOW 2016; 84: 292-314.

[7] YUAN, D.W., PAN, L.M., CHEN, D., ZHANG, H., WEI, J.H., and HUANG, Y.P.: Bubble behavior of high subcooling flow boiling at different system pressure in vertical narrow channel. APPL THERM ENG 2011; 31: 3512-20.

[8] YUAN, D., CHEN, D., YAN, X., XU, J., LU, Q., and HUANG, Y.: Bubble behavior and its contribution to heat transfer of subcooled flow boiling in a vertical rectangular channel. ANN NUCL ENERGY 2018; Vol.119: 191-202.

[9] XU, J.J., CHEN, B.D., WANG, X., and YAN, X.: Prediction of Sliding Bubble Velocity and Mechanism of Sliding Bubble Motion along the Surface. J ENHANC HEAT TRANSF 2010; 17.

[10] XU, J.J., CHEN, B.D., and WANG, X.J.: Study on bubble growth and departure near wall in vertical narrow rectangular channel. Atomic Energy Science & Technology 2010; 44: 1349-54.

[11] XU, J.J., CHEN, B.D., HUANG Y.P., YAN, X., and YUAN, D.W.: Experimental visualization of sliding bubble dynamics in a vertical narrow rectangular channel. Nuclear Engineering & Design 2013; 261: 156-64.

[12] YANG, K., CAO, X., YAN, C., YANG, Y., TIAN, C., and XU, J.: Visualization Study of Bubble Sliding Characteristics in a Subcooled Flow Boiling Narrow Rectangular Channel Under Natural Circulation Condition, 2017 25th International Conference on Nuclear Engineering. American Society of Mechanical Engineers, 2017: V9T-V15T.

[13] PULI, U., and ANIL KUMAR, R.: Parametric effect of pressure on bubble size distribution in subcooled flow boiling of water in a horizontal annulus. EXP THERM FLUID SCI 2012; 37: 164-70.

[14] MAURUS, R., ILCHENKO, V., and SATTELMAYER, T.: Study of the bubble characteristics and the local void fraction in subcooled flow boiling using digital imaging and analysing techniques. EXP THERM FLUID SCI 2002; 26: 147-55.

[15] ZENG, L.Z., KLAUSNER, J.F., BERNHARD, .D.M., and MEI, R.: A unified model for the prediction of bubble detachment diameters in boiling systems—II. Flow boiling. INT J HEAT MASS TRAN 1993; 36: 2271-9.

[16] KLAUSNER, J.F., MEI, R., BERNHARD, D.M., and ZENG, L.Z.: Vapor bubble departure in forced convection boiling. International Journal of Heat & Mass Transfer 1993; 36: 651-62.

[17] THORNCROFT, G.E., and KLAUSNER, J.F.: Bubble forces and detachment models. Multiphase Science & Technology 2001; 13: 35-76.

[18] COLOMBO, M., and FAIRWEATHER, M.: Prediction of bubble departure in forced convection boiling: A mechanistic model. International Journal of Heat & Mass Transfer 2015; 85: 135-46.

[19] ZEITOUN, O., and SHOUKRI, M.: Bubble Behavior and Mean Diameter in Subcooled Flow Boiling. Journal of Heat Transfer 1996; 118: 110-6.

[20] PARK, H., CHOI, K., CHO, S., YI, S., PARK, C., and CHUNG, M.: Experimental study on the natural circulation of a passive residual heat removal system for an integral reactor following a safety related event. ANN NUCL ENERGY 2008; 35: 2249-58.

[21] HA, K.S., PARK, R.J., KIM, H.Y., KIM, S.B., and KIM, H.D.: A study on the two-phase natural circulation flow through the annular gap between a reactor vessel and insulation system. INT COMMUN HEAT MASS 2004; Vol.31: 43-52.

[22] YANG, C., KAWARA, Z., YOKOMINE, T., and KUNUGI, T.: Visualization study on bubble dynamical behavior in subcooled flow boiling under various subcooling degree and flowrates. International Journal of Heat & Mass Transfer 2016; 93: 839-52.

[23] KLINE, S.J.: MFA. Describing Uncertainties in Single-Sample Experiments. Mech. Eng 1953; 75: 3-8.